5-2020

Trace Elements Cycling in a Crude Oil-Contaminated Aquifer near Bemidji, Northern Minnesota

Katherine Lane Jones
Trinity University, katherinej.98@gmail.com

TRACE ELEMENT CYCLING IN A CRUDE OIL-CONTAMINATED AQUIFER NEAR BEMIDJI, NORTHERN MINNESOTA

KATHERINE LANE JONES

A DEPARTMENT HONORS THESIS SUBMITTED TO THE

DEPARTMENT OF GEOSCIENCES AT TRINITY UNIVERSITY

IN PARTIAL FULFILLMENT OF THE REQUIREMENTS FOR GRADUATION WITH DEPARTMENTAL HONORS

APRIL 29, 2020

BRADY A. ZIEGLER
THESIS ADVISOR

KATHLEEN D. SURPLESS
DEPARTMENT CHAIR

Michael Soto, AVPAA

Student Agreement

I grant Trinity University (“Institution”), my academic department (“Department”), and the Texas Digital Library ("TDL") the non-exclusive rights to copy, display, perform, distribute and publish the content I submit to this repository (hereafter called "Work") and to make the Work available in any format in perpetuity as part of a TDL, digital preservation program, Institution or Department repository communication or distribution effort.

I understand that once the Work is submitted, a bibliographic citation to the Work can remain visible in perpetuity, even if the Work is updated or removed.

I understand that the Work's copyright owner(s) will continue to own copyright outside these non-exclusive granted rights.

I warrant that:

1) I am the copyright owner of the Work, or

2) I am one of the copyright owners and have permission from the other owners to submit the Work, or

3) My Institution or Department is the copyright owner and I have permission to submit the Work, or

4) Another party is the copyright owner and I have permission to submit the Work.

Based on this, I further warrant to my knowledge:

1) The Work does not infringe any copyright, patent, or trade secrets of any third party,

2) The Work does not contain any libelous matter, nor invade the privacy of any person or third party, and

3) That no right in the Work has been sold, mortgaged, or otherwise disposed of, and is free from all claims.

I agree to hold TDL, DPN, Institution, Department, and their agents harmless for any liability arising from any breach of the above warranties or any claim of intellectual property infringement arising from the exercise of these non-exclusive granted rights.”

I choose the following option for sharing my thesis (required):

[X] Open Access (full-text discoverable via search engines)

[ ] Restricted to campus viewing only (allow access only on the Trinity University campus via digitalcommons.trinity.edu)

I choose to append the following Creative Commons license (optional):

Abstract

Reduction of ferric (Fe(III)) hydroxides is an important electron accepting process within a crude oil-contaminated aquifer near Bemidji, MN, USA. Fe(III) hydroxides commonly sorb trace elements in aquifer sediments; when they are reductively dissolved, trace elements can be mobilized into groundwater. We present new analyses of spatial distribution in groundwater and in sediment that document the mobilization of barium (Ba), strontium (Sr), cobalt (Co), and nickel (Ni) from sediment into groundwater. In the most reducing zone of the aquifer, Ba, Sr, Co, and Ni concentrations are elevated in groundwater and depleted in sediments. Downgradient from this zone, supersaturation of groundwater with respect to Fe^{2+} and HCO_3^- leads to the precipitation of siderite, which sorbs Ba, Co, and Ni due to negative surface charge generated at the pH conditions in the Bemidji aquifer. At the transition zone between Fe(III) reducing conditions and (sub)oxic groundwater, hydrous ferric oxides precipitate, promoting sorption of Ba, Co, Ni, and Sr.

Results from mass balance modeling show that ≥99.5% of mass for each trace element is associated with sediment, both before and 40 years after the oil spill. However, mobilization into groundwater is associated with a 2x increase in Sr mass, 3x increase in Ba mass, 14x increase in Ni mass, and 33x increase in Co mass relative to the mass contained in uncontaminated groundwater. This dissolved mass was sufficient to exceed health advisory concentrations for Ba and Ni in drinking water. Our results highlight the importance of monitoring inorganic contaminants, and particularly trace elements, at organic contaminant sites.

Introduction

Naturally occurring trace elements are a common inorganic contaminant in groundwater. Several trace elements, including arsenic (As), barium (Ba), and nickel (Ni), are regulated at the national level by the United States Environmental Protection Agency (EPA), or recommended for regulation by the World Health Organization (WHO) due to their association with adverse health outcomes, which include elevated cancer risk, elevated blood pressure, gastrointestinal problems, and skin irritation (WHO reports). Other trace elements, such as aluminum, iron, and zinc, are subject to secondary regulations due to their aesthetic effects (odor, taste, appearance) on drinking water (US EPA). Additional trace elements, including cobalt (Co), strontium (Sr), and molybdenum (Mo) are presently unregulated but are on the EPA Contaminant Candidate

List, meaning that they are under consideration for future federal regulation due to their potential to occur in public drinking water systems at levels of public health concern (US EPA).

Monitored natural attenuation is often the most expedient approach to remediating aquifers affected by the release of organic contaminants. Microorganisms can oxidize (i.e., biodegrade) and consume the bioavailable organic carbon, and in doing so, they can transfer electrons to numerous electron acceptors via terminal electron accepting processes (TEAPs), which include oxygen consumption, nitrate reduction, manganese reduction, iron reduction, sulfate reduction, and methanogenesis. Recent research has demonstrated that Fe(III) reduction following the release of organic contaminants, including sewage plumes (Amirbahman et al., 2006), landfills (deLemos et al., 2006), crude oil releases (Cozzarelli et al., 2016; Ziegler et al., 2017a; Ziegler et al., 2017b), and petroleum/ethanol mixtures (Ziegler et al., 2015), can lead to the dissolution of arsenic (As) that was previously sorbed to Fe(III) hydroxides within aquifer sediments. These studies raised concerns about As concentrations in excess of the EPA drinking water standard (10 µg/L) due to this mobilization. This concern was exacerbated by the fact that regulations of organic-contaminated sites focus on the organic contaminant(s), and traditional monitoring at these sites does not include As and other inorganic contaminants that could be released as a secondary impact of natural attenuation.

This research focuses on a crude oil-contaminated aquifer located near Bemidji, MN, where long-term biodegradation has created anoxic and suboxic zones surrounding the primary contaminant plume (Tuccillo et al., 1999). In the anoxic zone of the aquifer, methanogenesis and Fe(III) reduction are the primary TEAPS that facilitate biodegradation (Cozzarelli et al., 2016). As a result of reductive dissolution of Fe(III) hydroxides, most (>78%) of adsorbed As within sediments near the oil source was mobilized into groundwater, creating dissolved As concentrations ≥23x the EPA drinking water standard near the contaminant plume (Ziegler et al., 2017a). However, mass balancing models indicate that this dissolved fraction represented only ~0.25-0.36% of total As mass within the contaminant plume (Ziegler et al., 2017b). Furthermore, a reactive transport model suggests that As concentrations >10 µg/L may persist in the Bemidji groundwater for more than 200 years (Ziegler et al., in review).

Modeling results indicate that if sorbed trace elements exist in sufficient quantities in aquifer sediments, even “minor” amounts of dissolution (<1%) following Fe(III) reduction may create toxic concentrations within groundwater given chronic exposure (Erickson & Barnes,

2005). Although research indicates that oil spills and other bioavailable organic matter sources have the potential to mobilize As into groundwater at toxic concentrations, there has been limited research on mobilization of other potentially toxic naturally occurring trace elements (i.e., Crow et al., 2007; Frierdich and Catalano, 2011; Ramos et al., 2014). In particular, few studies of trace element mobilization due to biodegradation are from a field setting. Our study uses new and archival field data from the Bemidji, MN crude oil contamination site to quantify the mobilization of Ba, Co, Ni, and Sr from aquifer sediments into groundwater.

Site Description

In 1979, a crude oil pipeline ruptured northwest of Bemidji, MN, releasing 10,700 barrels of crude oil onto a shallow glacial outwash aquifer. Despite clean-up efforts, ~25% of the crude oil infiltrated into the subsurface and pooled on the water table (USGS). Dissolution of hydrocarbons over time formed a dissolved contaminant plume.

In 1983, the spill site became a United States Geological Survey (USGS) sponsored research site through the Toxics Substances Hydrology Program, yielding an extensive (35+ year) historical record of biodegradation and other natural attenuation processes. The hydrogeologic and biogeochemical characterization of the Bemidji site (Lovley et al., 1989; Bennett et al., 1993; Baedecker et al., 1993; Tuccillo et al., 1999; see Essaid et al., 2011 for a summary of previous work) provides important data for studying the secondary processes occurring in an organic-contaminated aquifer.

The study site is located within the Pleistocene Bagley Outwash Plain (Bennett et al., 1993). The aquifer is ~20 meters thick, with a water table gradient of ~0.003; intercalated sand, silt, and gravel layers with high spatial heterogeneity overlie a clay-rich glacial till layer (Bennett et al., 1993). Although groundwater velocities in the majority of the aquifer range from 0.15 to 0.5 m/d, velocity is as low as 0.05 m/d in silty layers (Bennett et al., 1993). On average, aquifer sands are 60% quartz, 5% carbonates, 30% feldspars, and ~5% heavy minerals (including hornblende and ilmenite); silts have a significantly higher carbonate content than coarser-grained sediments (Bennett et al., 1993). Total iron content in uncontaminated sediments is ~1 wt% distributed across a complex mineral suite, with approximately 50% in ferrous iron phases (Zachara et al., 2004).

Table 1.
Relevant biodegradation reactions at the Bemidji aquifer. Adapted from Ng et al. (2014) and Cozzarelli et al. (2016).

Reaction Name	Equilibrium Reaction	Effects	Zone in Aquifer
Aerobic Degradation	$C_6H_6 + 7.5O_2 + 3H_2O \rightarrow 6HCO_3^- + 6H^+$	Anoxia, increased acidity, increased alkalinity	III, I-II (historically)
Fe(III) Reduction	$C_6H_6 + 30Fe(OH)_{3(s)} + 54H^+ \rightarrow 6HCO_3^- + 30Fe^{2+} + 72H_2O$	Dissolved Fe^{2+}, dissolved trace elements, reduced acidity, increased alkalinity	II, I (historically)
Methanogenesis	$C_6H_6 + 6.75H_2O \rightarrow 2.25HCO_3^- + 3.75CH_4 + 2.25H^+$	Increased acidity	I

Long-term biodegradation has created five geochemical zones proceeding downgradient from the oil pool (Cozzarelli et al., 2016). The anoxic region is subdivided into two zones: (I) the methanogenic zone, which was previously Fe-reducing but became predominantly methanogenic due to depletion of bioavailable Fe(III) in sediments, and (II) the anoxic Fe-reducing zone. The presence of organic acids (from the crude oil) and acidity produced via methanogenesis (Ng et al., 2014) result in pH values ~1 unit lower than in uncontaminated groundwater (Bennett et al., 1993). In both Zone I and Zone II, benzene, Fe^{2+}, and As concentrations are high due to biodegradation and reductive dissolution (Cozzarelli et al., 2016). In Zone III, the suboxic transition zone between the contaminant plume and uncontaminated groundwater, dissolved Fe concentrations return to background levels as Fe^{2+} oxidizes and precipitates in the form of Fe(III) hydroxides at the leading edge of the contaminant plume (Cozzarelli et al., 2016). The precipitated hydrous ferric oxides in Zone III attenuate the As contaminant plume in Zones I and II via sorption (Ziegler et al., 2017b), and may have a similar effect on other dissolved trace elements. Zone III grades into Zone IV, the oxic background waters, which is underlain by Zone V, the naturally sub-oxic groundwater beneath the lower plume boundary; benzene, dissolved Fe, and dissolved As concentrations are low or negligible in both zones (Cozzarelli et al., 2016).

This study uses new and archival groundwater and sediment data from the Bemidji site to identify plumes of mobilized Ba^{2+}, Co^{2+}, Ni^{2+}, and Sr^{2+} that resemble previously identified Fe

and As contaminant plumes. Via mass balance modeling, we compare background sediment and groundwater concentrations with the concentrations within the contaminated zone in order to quantify the degree of mobilization and sediment-groundwater repartitioning for each trace element.

Materials and Methods

Groundwater Sample Collection and Analysis

Groundwater samples were collected annually from 2010 to 2019 along the center-line transect of the hydrocarbon plume (Figure 1). Wells containing free oil product were sampled with a Teflon bailer, and the aqueous and NAPL phases were allowed to partition via gravity. Only aqueous concentrations are reported in our study. Wells absent of free oil product were sampled using a submersible Keck pump. A minimum of three well volumes were pumped prior to sampling, and samples were collected after field parameters (temperature, pH, dissolved oxygen, and specific conductance) were stable. Samples were analyzed for a standard trace element suite (Li, Be, B, Al, V, Cr, Mn, Co, Ni, Cu, Rb, Sr, Mo, Ag, Cd, Sb, Sn, Zn, Mg, Se, Cs, Ba, La, Ce, Tl, Pb, B, Th, U, Li, Zn) using inductively coupled plasma mass spectrometry (ICP-MS). Major and minor elements (Ca, Na, Mg, K, Si, Sr, Al, Fe, Mn, B, Ba, Li, Cu, Zn) were quantified via inductively coupled plasma optical emission spectrometry (ICP-OES). Representative groundwater concentrations for each element in each well were determined by selecting the highest concentration measured in the 2010-2019 dataset that was not rejected as a statistical outlier.

Sediment Collection, Digestion, and Analysis

Sediment cores were collected in 2014, 2015, 2016, and 2019 (Figure 1). Cores were collected via drilling approximately 0.3 m below the water table (8-11 m below land surface) with a hollow-stem auger, and pounding a 2.1 m piston core barrel beneath the augers. To preserve the record of subsurface geochemistry, the bottom 10 centimeters of the core barrel were frozen with liquid CO_2 *in situ* (Murphy & Herkelrath, 1996). Immediately following extraction, core ends were covered in plastic wrap and capped. Cores were then logged for physical description and cut into sub-sections, which were also wrapped and capped. Sub-sections were then wrapped in foil, vacuum-sealed in bags, and frozen onsite. Cores were

shipped with dry ice to either the U.S. Geological Survey in Reston, VA, Virginia Tech in Blacksburg, VA, or Trinity University in San Antonio, TX.

In the laboratory, samples were removed from core sub-sections in an anaerobic chamber (or in open air if redox preservation was not a priority).Samples were dried in an oven for 24 hours at 40°C, then ground lightly with a mortar and pestle. Grain sizes >2 mm were removed using forceps. Samples were then digested using trace metal-grade nitric acid via microwave-assisted digestion (EPA Method 3051a). Extracts were diluted 1:10 or 1:50 with nanopure water and analyzed for a standard trace element suite using both ICP-OES and ICP-MS.

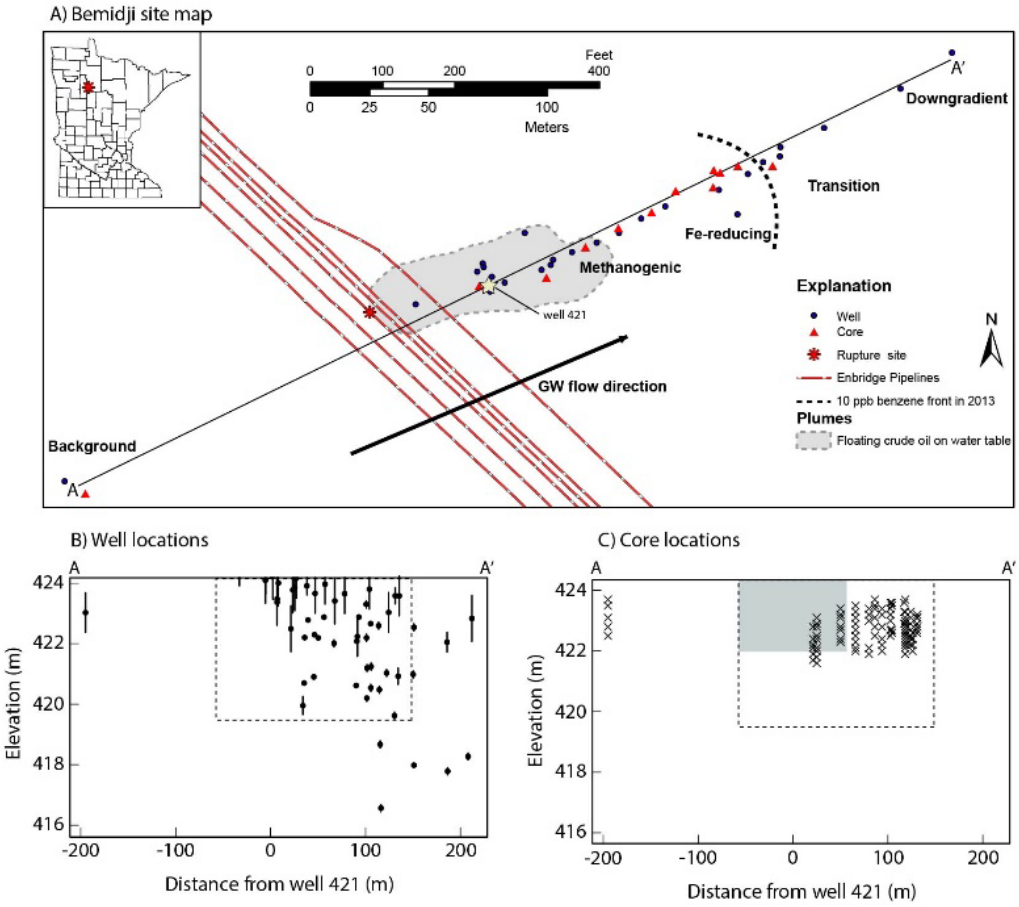

Fig. 1. A) Map of the Bemidji spill site showing locations of cores and wells sampled for this study (easting 342,785, northing 5,271,040, UTM zone 15N North American Datum 1983). Inset shows site location within Minnesota. B) Cross section view of wells sampled; circles correspond to the center of the screen and vertical lines indicate the full screen length. The dashed rectangle denotes the plume domain used for mass balance modeling. C) Cross section view of sediment sampling locations. Well 421 is the historical zero reference point for plume transects across the center of the oil body. Figure modified from Ziegler et al. (2017b).

Statistical Analysis

For wells that were sampled multiple times between 2010 and 2019, the element concentration was used unless rejected by a Grubbs' Test for outliers. Outliers in sediment and groundwater samples were analyzed via Grubbs' test for outliers (Grubbs, 1950):

$$G = \frac{|C_{max} - \bar{C}|}{s}$$

where G is the Grubbs' test statistic, C_{max} is the maximum reported concentration in the sample set of interest, $\bar{C}$ is the mean sample concentration, and s is the sample standard deviation. If a groundwater sample concentration was rejected by a Grubbs' test for outliers, but was associated with multiple elevated concentrations, we did not exclude it from the dataset.

Mass Balance Design

The mass balance design for this study follows the procedure outlined in Ng et al. (2014) and modified in Ziegler et al. (2017b). Mass balance calculations assume conservation of mass within the domain boundaries, and that partitioning occurred exclusively between sediment and groundwater phases (i.e., that mass did not volatilize or incorporate into biomass). Under these assumptions, the following equation was used for each separate trace element:

$$mass_{pre\text{-}spill\ groundwater} + mass_{pre\text{-}spill\ sediment} = mass_{present\ groundwater} + mass_{present\ sediment}$$

where pre-spill masses are represented by background well and sediment core data, and "present" masses represent the mass of a given trace element from 2014-2019 sediment and groundwater samples.

All Ba, Co, Ni, and Sr data from sediment and groundwater were assigned to a cross-sectional domain grid across the plume transect. Domain boundaries were 200 meters upgradient to 220 meters downgradient of well 421 (the center of the oil body and historic reference point at the Bemidji site), and 416 meters to 424 meters in elevation above mean sea level. The domain was gridded with a cell size of 1.5 meters horizontal by 0.5 meters vertical, for a total of 4480 cells.

Based on the gridding method and some well screen lengths, well screens at the Bemidji site sometimes span multiple domain grid cells. To address this issue, Ziegler et al. (2017b)

applied two different methods: 1) assign the measured trace element mass only to the cell intersected by the center of the well screen, and 2) assign the measured trace element mass to all cells intersected by the well screen. Differences between the two methods were insubstantial, and we applied the method using the center of screen only in this study.

Plume boundaries were delineated within the model domain based on the similar spatial distributions of the trace element plumes as compared to the As and Fe plumes described by Ziegler et al. (2017b). This plume domain is -60.5 m to 151 m from well 421, and 419.5 m to 424 m in elevation, for a total of 1260 cells; groundwater concentrations for relevant elements are relatively low or non-detectable outside of these domain boundaries. To account for sparse data beneath and adjacent to the oil body, we followed the method of Ng et al. (2014) and assumed that these regions would resemble the most reducing regions of the aquifer. For groundwater, we applied values corresponding to the 90^{th} percentile of concentrations measured for each trace element to the upgradient lower and upper corners of the plume rectangle. For sediment, we applied the mean concentrations for each trace element in the most reducing zone of the plume (5-25 m from well 421) to the rectangle corners.

Because the aquifer sediments are primarily quartzose, we used the density of quartz (2.65 g/cm^3) to convert element concentrations in sediment (mg/kg) to mass units. Groundwater and sediment concentrations of each element (g/m^3) were interpolated over the domain grid using linear kriging in Surfer 11 (Golden Software). Then, the groundwater and sediment concentrations for each element were integrated over the area within the plume boundary, yielding a calculation of the mass per meter of aquifer thickness (g/m, oriented perpendicular to the direction of groundwater flow).

Results

Trace Elements of Interest

Samples were analyzed for a standard trace element suite (Li, Be, B, Al, V, Cr, Mn, Co, Ni, Cu, Rb, Sr, Mo, Ag, Cd, Sb, Sn, Zn, Mg, Se, Cs, Ba, La, Ce, Tl, Pb, B, Th, U, Li, Zn) using inductively coupled plasma mass spectrometry (ICP-MS) for groundwater and sediment samples and inductively coupled optical emission spectrometry (ICP-OES) for sediment samples. Of the trace elements analyzed, Ba^{2+}, Sr^{2+}, Co^{2+}, and Ni^{2+} showed discernable plumes in groundwater and sediment concentrations.

Background Values in Sediment and Groundwater

Table 2 reports measured values for Ba, Sr, Co, and Ni in sediment and groundwater samples collected upgradient and far downgradient (for groundwater) from the plume boundaries. Well samples downgradient of the plume were considered to be "background" samples if they were more than 200 m downgradient from well 421, within oxic conditions and beyond the leading edge of dissolved trace element fronts. Grubbs' test identified several sediment samples as outliers (2 for Ba(II) and 1 each for Sr(II), Co(II), and Ni(II); denoted ** in Table 2) due to abnormally high trace element concentrations; these outliers were omitted in calculations of background sediment values.

Table 2.
Background sediment and groundwater chemistry. Values denoted ** are outliers and not included in statistical calculations. Because of the COVID-19 pandemic, our sediment samples have not been analyzed and reported by the contract laboratory, and thus the sediment data is incomplete; values that are yet to be reported (or are otherwise absent, in the case of groundwater data) are denoted --. Concentrations less than the analytical limit of detection are reported as BDL (below detection limit), and statistical information is reported as zero (after rounding).

Core Samples					
Location	Elevation (m AMSL)	Ba (mg/kg)	Co (mg/kg)	Ni (mg/kg)	Sr (mg/kg)
upgradient	422.43	13.99	--	--	--
upgradient	422.43	8.96	1.31	2.96	12.51
upgradient	422.59	19.39	--	--	20.59
upgradient	422.62	13.99	--	--	--
upgradient	422.74	37.42**	--	--	43.57**
upgradient	422.78	20.20	--	--	--
upgradient	423.08	8.06	2.10	5.00	18.44
upgradient	423.10	23.20	--	--	24.80
upgradient	423.54	14.39	3.82	6.90	30.62
upgradient	423.72	16.31	2.59	5.12	16.16
upgradient	423.72	20.19	3.53	6.81	22.79
upgradient	423.73	9.03	1.92	4.54	19.61
upgradient	423.76	38.00**	4.36**	9.38**	21.60
upgradient	423.76	32.41	3.32	7.63	19.65

upgradient	424.15	15.22	2.21	4.58	13.63
upgradient	424.15	17.40	2.09	4.16	12.62
	Mean	16.62	2.54	5.30	19.42
	Standard deviation	6.43	0.84	1.51	5.32
	25^{th} percentile	11.51	1.97	4.55	16.16
	75^{th} percentile	20.19	3.42	6.85	22.49

Groundwater Samples					
Location	Elevation (m AMSL)	Ba^{2+} (µg/L)	Co^{2+} (µg/L)	Ni^{2+} (µg/L)	Sr^{2+} (µg/L)
upgradient	406.89	139	BDL	3.0	198
upgradient	423.05	393	BDL	3.0	63
upgradient	424.34	62	BDL	2.0	75
downgradient	419.88	56	--	--	--
downgradient	418.30	67	1.2	2.9	83
downgradient	422.94	75	BDL	2.6	102
downgradient	420.24	201	--	--	58
downgradient	419.19	64	BDL	0.8	79
downgradient	424.24	34	BDL	0.3	58
downgradient	420.27	78	BDL	0.5	90
downgradient	421.40	67	BDL	0.7	85
	Mean	112	0	1.8	89
	Standard deviation	63	0	0.7	66
	25^{th} percentile	77	0	2.7	85
	75^{th} percentile	104	0	1.2	41

Spatial Distribution of Mass in Sediment and Groundwater

Mean background sediment and groundwater concentrations for Ba^{2+}, Co^{2+}, Ni^{2+}, and Sr^{2+} (see Table 2) were applied uniformly over the domain grid. Calculated sediment masses for the entire model domain were 26 kg/m for Ba(II), 30.4 kg/m for Sr(II), 3.98 kg/m for Co(II), and 8.29 kg/m for Ni(II) (Table 3). Based on groundwater background values, Co^{2+} concentrations were below detection (<0.5 µg/L) prior to the oil spill, so a value of 0 kg/m was applied to the

aqueous phase for mass balance purposes. Ba^{2+}, Sr^{2+}, and Ni^{2+} had detectable background groundwater concentrations of 112 µg/L for Ba, 89 µg/L for Sr, and 1.8 µg/L for Ni, yielding domain totals of 0.041 kg/m, 0.032 kg/m, and 0.0006 kg/m, respectively. The 25th and 75th percentiles of background sediment sample concentrations provided a range of uncertainty in domain totals.

Table 3.

Mass balance results.

Ba Mass Balance		Mass kg/m (uncertainty)	Percent of domain total
Prior to oil spill	Groundwater	0.041	0.2
	Sediment	26 (18-31.6)	99.8
	Total	26.041 (18.041-31.641)	100
Current (40 years after oil spill)	Groundwater	20.9	80.3
	Sediment	0.108	0.4
	Total	21.08	80.7
Sr Mass Balance			
Prior to oil spill	Groundwater	0.032	0.1
	Sediment	30.4 (25.3-35.2)	99.9
	Total	30.432 (25.332-35.232)	100
Current (40 years after oil spill)	Groundwater	0.061	0.2
	Sediment	28.5	93.9
	Total	28.561	94.1
Co Mass Balance			
Prior to oil spill	Groundwater	0	0
	Sediment	3.98 (3.07-5.35)	100
	Total	3.98 (3.07-5.35)	100
Current (40 years after oil spill)	Groundwater	0.003	0.1
	Sediment	2.24	56.2
	Total	2.243	56.3
Ni Mass Balance			
Prior to oil spill	Groundwater	0.0006	0.01
	Sediment	8.29 (7.11-10.7)	99.99
	Total	8.2906 (7.1106-10.7006)	100
Current (40 years after oil spill)	Groundwater	0.0089	0.11
	Sediment	5.05	60.89
	Total	5.0589	61.0

The kriged sediment element concentrations across the plume domain indicate redistribution of Ba(II), Sr(II), Co(II), and Ni(II) mass associated with biodegradation of hydrocarbons over the past 40 years (Figure 2). Co(II) and Ni(II) are substantially depleted in

sediments beneath and adjacent to the oil body, and Ba(II) and Sr(II) values are below background concentrations downgradient from the oil body. Zones of enrichment occur downgradient from and adjacent to these depleted regions, and are spatially heterogeneous (Figure 2). Maximum sediment concentrations represent up to a 57% increase relative to background mass for Ba(II), up to a 51% increase relative to background mass for Sr(II), up to a 18% increase relative to background mass for Ni(II), and up to a 9% increase relative to background mass for Co(II). Maximum sediment concentrations form a "wall" at ~80 m downgradient from well 421 for Ba(II), Co(II), and Ni(II) (Figure 2). A second "wall" of elevated sediment concentrations occurs at ~110 m downgradient for Ba(II), Sr(II), and to a minor extent Co(II) and Ni(II) (Figure 2).

The kriged groundwater element concentrations demonstrate that groundwater is enriched in Ba^{2+}, Co^{2+}, Ni^{2+}, and Sr^{2+} in the plume region relative to the background regions, though each trace element exhibits different spatial distributions (Figure 2). The maximum concentration in groundwater samples was 794 µg/L for Ba^{2+} (7x greater than mean background value), 281 µg/L for Sr^{2+} (3x greater than mean background value), 29 µg/L for Co^{2+} (116x greater than mean background value), and 118 µg/L for Ni^{2+} (66x greater than mean background value). For Ba^{2+}, Sr^{2+}, Co^{2+}, and Ni^{2+}, the highest groundwater concentrations occur near well 421, beneath the oil body. Co^{2+} and Ni^{2+} concentrations decrease along the flowpath and with depth, returning to background values by ~70 m downgradient of well 421 (Figure 2). Elevated Ba^{2+} and Sr^{2+} concentrations are comparatively persistent and spatially heterogeneous across the plume region. For both elements, the leading edge of the plume occurs at ~150 m downgradient of well 421, but in the Ba^{2+} plume, groundwater concentrations decrease somewhat between ~75 m downgradient from well 421 and the leading edge of the plume (Figure 2).

Comparisons of pre-spill estimates and present-day mass balance calculations indicate that dissolved mass in the model domain approximately doubled for Sr, tripled for Ba, increased 14 times for Ni, and increased 33 times for Co. Although these are substantial increases, calculations for present-day groundwater Ba^{2+}, Co^{2+}, Ni^{2+}, and Sr^{2+} masses account for only 0.1-0.4% of pre-spill mass estimates. The amount of dissolved mass accounted for in present-day domain totals also varies by element. When pre-spill domain totals are calculated using mean background concentrations, 6% of Sr mass, 19% of Ba mass, 39% of Ni mass, and 44% of Co mass is unaccounted for in current estimates.

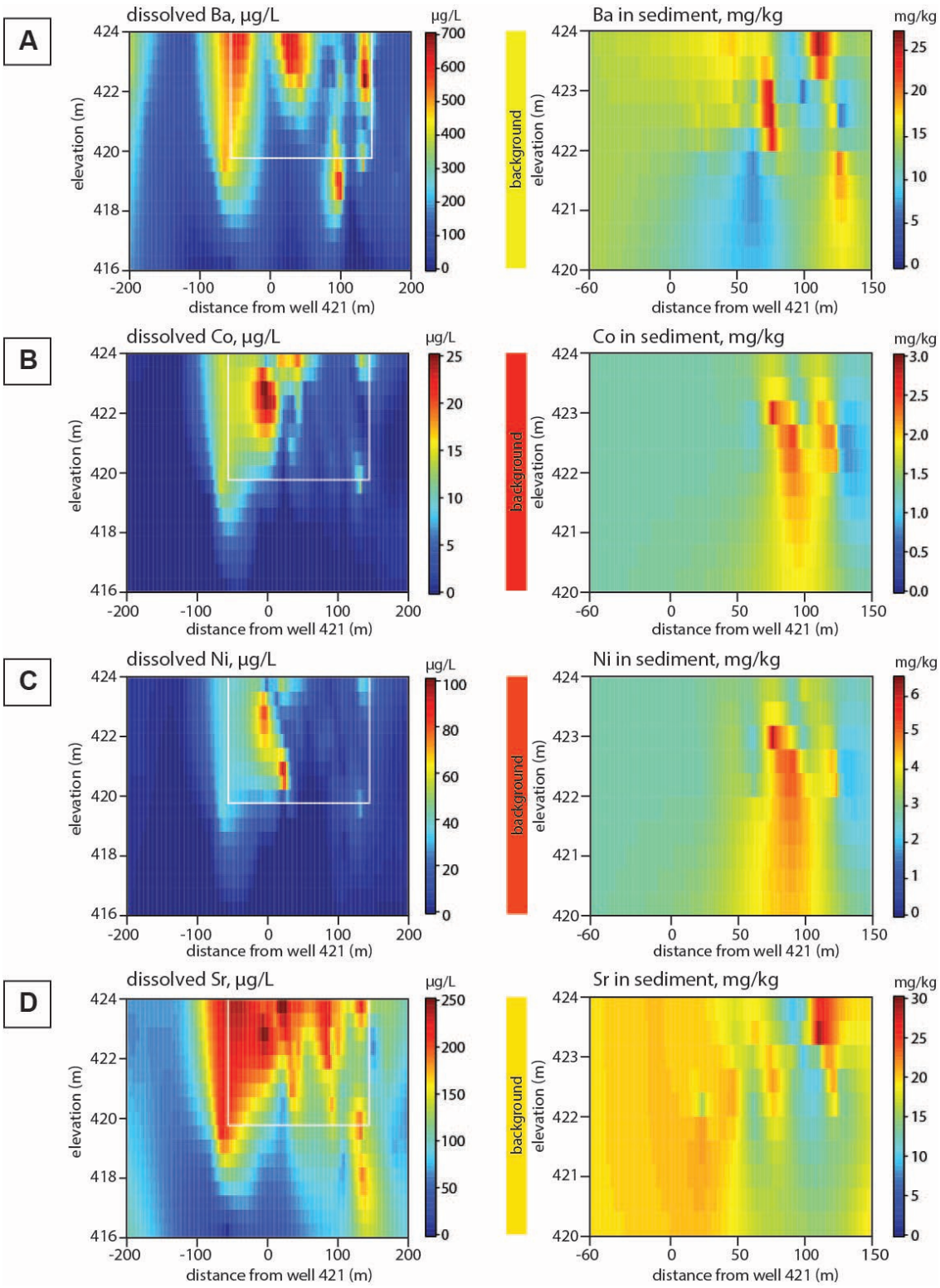

Fig. 2. Kriged groundwater (left, in µg/L) and sediment (right, in mg/kg) concentrations for A) barium, B) cobalt, C) nickel, and D) strontium in the Bemidji aquifer. The white rectangle in the groundwater concentration maps outlines the plume boundaries used for mass balance modeling.

An estimate for the degree of mobilization from sediment into groundwater for each element was quantified by calculating the percentage of pre-spill cell mass (in kg/m) represented by the average sediment mass in the most reducing zone of the aquifer (5-25 m downgradient from well 421); pre-spill groundwater mass was sufficiently low that it did not affect this calculation. These calculations indicated that 49% of Co mass, 46% of Ni mass, and 21% of Ba mass was mobilized from the most contaminated region of the Bemidji aquifer (the average Sr mass in this zone exceeded pre-spill cell mass and this calculation was therefore ineffective at quantifying the degree of Sr mobilization).

Discussion

Variation in Spatial Distribution of Trace Element Masses

This study documents zones of elevated Ba, Co, Ni, and Sr concentrations in groundwater, and depleted concentrations in sediment, adjacent to the oil body in the Bemidji aquifer. These zones are similar to the Fe and As plumes documented in previous research (Cozzarelli et al., 2016; Ziegler et al., 2017a; Ziegler et al., 2017b), and also feature regions of elevated sediment concentrations near the leading edge of the plume, where anoxic waters mix with (sub)oxic groundwater. Interestingly, there is heterogeneity in the regions of elevation in sediment. For example, there is a "wall" of sediment enriched in Co(II), Ni(II), and Ba(II) at ~80-90 m downgradient from well 421; because this region is actively Fe-reducing and therefore hydrous ferric oxide (HFO) minerals are depleted, trace element precipitation into sediment is unexpected. A second wall of enrichment occurs for Ba(II) and Sr(II), and to a lesser extent Co(II) and Ni(II), at ~110-120 m downgradient from well 421. At this interface, dissolved Fe^{2+} oxidizes, forming HFO precipitates that create a zone of elevated concentration in sediments that extends from ~110-130 m downgradient from well 421 (Ziegler et al., 2017b). This Fe(III)-rich zone has a higher sorption capacity to remove dissolved trace elements, including As, Ba^{2+}, Sr^{2+}, Co^{2+}, and Ni^{2+} via surface complexation reactions, although the zones of elevated sediment concentration for each element differs somewhat from the Fe zone.

Ba, Co, Ni, and Sr mass balances document the mobilization of mass from sediment into groundwater. However, plume geometries vary for each element. Ni and Co plumes in groundwater are centered on well 421 and largely conform to the boundaries of the most reducing region of the contaminant plume. In the most reducing region of the plume, 5-25 m downgradient from well 421, Co and Ni masses in sediment are roughly one half of background

or pre-spill mass values. Co and Ni masses partition back to the sediments ~80-90 m downgradient from well 421, although resorption onto iron oxide minerals is unlikely under the reducing conditions in this zone. In contrast, Ba and Sr are more persistent in groundwater and occur in heterogeneous zones within the plume, with leading edges extending as far as ~150 m downgradient from well 421. Zones of depleted Ba and Sr in sediment occur 50 m downgradient from well 421, outside of the most reducing region of the plume. The majority of Ba and Sr resorption appears to occur ~110 m downgradient from well 421, approximately 20 m further along the flowpath than the Co and Ni resorption zone, although some sorption appears to occur earlier at ~80-90 m downgradient from well 421.

Some of the variation between Ba/Sr and Co/Ni distributions in sediment and groundwater may be attributed to visualization methods. The maximum (non-outlier) concentrations observed in aquifer sediments were 3.8 mg/kg for Co, 8.1 mg/kg for Ni, 30.8 mg/kg for Sr, and 32.4 mg/kg for Ba. Mean background concentrations in sediments were 2.5 mg/kg for Co, 5.3 mg/kg for Ni, 16.6 mg/kg for Ba, and 19.4 mg/kg for Sr. Both maximum and background Ba and Sr concentrations are an order of magnitude higher than Co and Ni maximum and background concentrations. These baselines for comparison yield visually dissimilar concentration interpolation maps; the same 1-2 mg/kg loss of mass translates to a relatively low percent mobilization for Ba, but constitutes a 40-50% mobilization for Co or Ni. Variation in scale of sediment concentration also provides a partial explanation for why present-day domain totals account for a more complete mass balance for Ba/Sr relative to Co/Ni mass between pre- and post-spill calculations.

Additionally, Ba and Sr have similar geochemical properties that differ slightly from Co and Ni, which have highly similar geochemical behaviors. These differences likely influence the spatial distributions observed in sediment and in groundwater. A study of alkaline earth cation (Ca, Sr, Ba, Ra) sorption demonstrated that the retention of Ba and Sr (and Ca and Ra) on biotite systematically decreases as ionic strength increases (Soderlund et al., 2019). Other researchers (Small et al., 2001) found that Sr sorption onto hydrous ferric oxides (HFO) is independent of ionic strength, but sorption onto bacteria-HFO composite solids has a moderately negative relationship with ionic strength. Research on the Bemidji plume (Ziegler et al., 2017a) suggested that As may sequester in silty layers at higher rates relative to sandy sediments due to

groundwater residence times and greater sorption capacity; it is possible that the same finer-grained, silt-rich layers also exhibit differential sorption of Ba/Sr or Co/Ni.

To explain the spatial variability of the various trace elements reported here and in Ziegler et al. (2017b), we invoke cation sorption onto Fe oxides using the electrical double layer model. This equilibrium-based model explains sorption based on physical sorbent properties (surface area, surface site density) and geochemistry at the mineral-solution interface (pH, ionic strength, elemental composition, etc.) (Dzombak & Morel, 1990). Sorption of each cation in solution is expressed as a thermodynamic expression with its own intrinsic surface complexation constant, derived from the literature and compiled by Dzombak and Morel (1990).

Table 4.
Surface complexation reactions between HFO and Ba^{2+}, Sr^{2+}, Co^{2+}, and Ni^{2+}, adapted from Dzombak & Morel (1990). Superscripts on Fe correspond to strong (inner layer) and weak (outer layer) sorption onto the HFO molecule, according to the electrical double layer model.

	Surface Complexation Reaction	Log K_1^{int}	Log K_2^{int}	Log K_3^{int}
Ni	$\equiv Fe^sOH^0 + Ni^{2+} = \equiv Fe^sONi^+ + H^+$	0.37	--	--
Co	$\equiv Fe^sOH^0 + Co^{2+} = \equiv Fe^sOCo^+ + H^+$	-0.46	--	--
	$\equiv Fe^wOH^0 + Co^{2+} = \equiv Fe^wOCo^+ + H^+$	--	-3.01	--
Sr	$\equiv Fe^sOH^0 + Sr^{2+} = \equiv Fe^sOHSr^{2+}$	5.01	--	--
	$\equiv Fe^wOH^0 + Sr^{2+} = \equiv Fe^wOSr^+ + H^+$	--	-6.58	--
	$\equiv Fe^wOH^0 + Sr^{2+} + H_2O = \equiv Fe^wOSrOH^0 + 2H^+$	--	--	-17.60
Ba	$\equiv Fe^sOH^0 + Ba^{2+} = \equiv Fe^sOHBa^{2+}$	5.46	--	--

Experimental data suggest that Co^{2+} (and likely Ni^{2+} by extension) has a higher type 1 site density than Sr^{2+}, corresponding to higher availability of cation-specific binding sites (Dzombak & Morel, 1990). Ba^{2+} and Sr^{2+} have higher intrinsic surface complexation constants than Co^{2+} and Ni^{2+}; furthermore, surface complexation models indicate that alkaline earth cations, including Ba^{2+} and Sr^{2+}, are capable of sorption to both protonated and deprotonated sites, whereas Co^{2+} and Ni^{2+} sorb to deprotonated sites (Dzombak & Morel, 1990). The pH_{50}, defined as the pH at which 50% of a dissolved trace element sorbs to HFO, is 6.6-6.7 for Co^{2+}, 6.6 for Ni^{2+}, 7-8.5 for Sr^{2+}, and 7.6-8.5 for Ba^{2+} (Dzombak & Morel, 1990). Additionally, research (Dzombak & Morel, 1990; Fischer et al., 2007) has documented a positive relationship

between metal affinity for hydroxide ions and metal affinity for goethite surface complexation. Co^{2+} and Ni^{2+} have higher equilibrium constants for aqueous complexation with hydroxyl ions as compared to Ba^{2+} and Sr^{2+} (Dzombak & Morel, 1990).

For hydrous ferric oxide surface complexation, Co^{2+} and Ni^{2+} have lower pH_{50} values, higher affinity for aqueous complexation with hydroxyl ions, and higher type 1 site densities as compared to Ba^{2+} and Sr^{2+} (Dzombak & Morel, 1990). Although Ba^{2+} and Sr^{2+} have higher sorption equilibrium constants, the elevated ionic strength of groundwater near the contaminant plume may hinder their capacity to sorb to ferric oxides (Soderlund et al., 2019), particularly if these ferric oxides are associated with bacteria (Small et al., 2001).

Additionally, hydrous ferric oxides may not be the only species capable of sorbing cations. Scanning electron micrograph images documented the presence of ferroan calcite, or siderite, within sediments in the contaminant plume zone of the Bemidji aquifer (Tuccillo et al., 1999). In Zone I of the aquifer, the presence of organic acids and acidity produced by both methanogenesis and historical aerobic degradation (see Table 1) dissolves carbonate minerals, resulting in high concentrations of HCO_3^- and CO_3^{2-} ions (Ng. et al, 2014). In Zone II, Fe(II) reduction consumes acidity and produces both HCO_3^- and Fe^{2+} ions (see Table 1). Under these geochemical conditions, siderite can precipitate by the following reaction:

$$Fe^{2+} + {CO_3}^{2-} = FeCO_{3(s)}$$

Saturation index values calculated by Ng et al. (2014) suggest that a zone of siderite precipitation occurred ~80 m downgradient from well 421 between 10-20 years after the oil spill, and ~100 m downgradient from well 421 approximately 30 years after the oil spill. Siderite has a PZNC of 5.3 (Charlet et al., 1990), meaning that at pH > 5.3, siderite surfaces generate negative surface charge and are therefore able to sorb cations from solution. The pH in the Bemidji aquifer ranges from 6-8, so siderite precipitated under these conditions would have a predominantly negative surface charge. This likely explains why there is a "wall" of cation sorption in the Fe-reducing zone, but not an analogous wall for As (Ziegler et al., 2017a), which exists as various oxyanions in solution and therefore will not sorb unless positive surface charge is generated.

A combination of siderite sorption and hydrous ferric oxide sorption may partially explain why Co^{2+} and Ni^{2+} resorb ~20 m closer than Ba^{2+} and Sr^{2+} along the flowpath from the hydrocarbon contaminant plume. As groundwater acidity decreases at the transition between

methanogenic and Fe(III)-reducing zones, supersaturation with respect to both HCO_3^- and Fe^{2+} favors the precipitation of siderite (Equation 1; Ng et al., 2014). Because Co^{2+} and Ni^{2+} have lower pH_{50} values compared to Ba^{2+} and Sr^{2+} (Dzombak & Morel, 1990), geochemical conditions favor their sorption under the somewhat acidic conditions (pH ~7) in this zone (Ng. et al., 2014); as such, elevated Co(II) and Ni(II) concentrations in sediments ~90 m downgradient from well 421 may indicate their preferential sorption onto siderite (Figure 2). Further down the flowpath, as pH continues to increase (up to ~7.3-7.5; Ng et al., 2014), ionic strength decreases, and redox conditions favor Fe(III) precipitation, Ba^{2+} and Sr^{2+} are favored to sorb to HFO precipitates due to their higher intrinsic surface complexation constants and ability to sorb to both protonated and deprotonated surface sites (Dzombak & Morel, 1990).

Missing Mass

Mass balance models in this study use mean background sediment concentrations, and fail to account for between 6% (Sr) and 44% (Co) of total pre-spill masses. Some of this mass may be accounted for by adjusting the background sediment concentration used to represent pre-spill aquifer sediments. When the 25th percentile background sediment concentration is used to calculate domain totals instead of the 50th percentile, current mass balance totals for Ba and Sr more than account for pre-spill masses, but 27% of Co mass and 29% of Ni mass remains unaccounted for. Another likely factor is the previously discussed difference in scale between Ba/Sr and Co/Ni, where Co and Ni mass balance models are more sensitive to the same amount of unaccounted for mass (e.g. 1 kg/m) due to containing substantially less total domain mass. Finally, our sampling regime likely fails to represent the full spatial heterogeneity of the contaminated aquifer. Limitations in core sampling technology mean that sediment cores do not fully capture the vertical boundaries of the contaminant plume, where anoxic plume waters mix with oxic groundwater recharge (upper boundary) and naturally (sub)oxic groundwater (lower boundary), both of which likely promote the oxidation of aqueous Fe^{2+} in the plume to form Fe(III) precipitates. Tuccillo et al. (1999) documented a zone of elevated Fe(III) in sediment along the lower plume boundary, which suggests that HFO precipitation and subsequent trace element sorption also occurs in this zone.

Mass Partitioning

As with As and Fe over the same domain (Ziegler et al., 2017b), sediment contains the vast majority (>99%) of Ba, Co, Ni, and Sr mass in the plume region. Although elevated dissolved trace element concentrations are 2-25 times higher than in background groundwater samples, dissolved mass accounts for <0.5% of the present-day, post-spill domain total. Maximum groundwater concentration values exceed the 70 µg/L EPA Health Advisory Drinking Water Equivalent Level for Ni^{2+} (EPA, 2018) and the 700 µg/L WHO guideline value for Ba^{2+} in drinking water (although Ba^{2+} concentrations do not exceed the 2 mg/L EPA MCL). Reported Ba(II) levels in soil generally range from 15 to 3500 mg/kg and Ni(II) levels range from 4 to 80 mg/kg (CDC Toxicological Reports); background sediment concentrations in the Bemidji aquifer (16.62 mg/kg for Ba(II) and 5.30 mg/kg for Sr(II)) are on the low end of both ranges. As such, mass balance models for Ba and Ni at the Bemidji site suggest that the majority of aquifers containing even low concentrations of Ba and Ni are vulnerable to groundwater concentrations of health concern of these elements, if organic matter biodegradation processes result in reducing geochemical conditions.

Conclusions and Implications

At the Bemidji aquifer site, reducing geochemical conditions result in the dissolution of Fe(III) hydroxides, which are associated with substantial increases in Ba^{2+}, Sr^{2+}, Co^{2+}, and Ni^{2+} groundwater concentrations due to mobilization from trace elements into groundwater. Although aquifer sediments remain the primary reservoir for trace element mass (>99.5% of Ba, Sr, Co, and Ni mass), spatial distributions indicate trace element depletion within sediments in the most reducing zones of the aquifer, and elevated concentrations in sediments downgradient from the contaminant zone. These elevated concentrations in sediment correspond to zones where geochemical conditions favor the precipitation of siderite, and subsequent sorption of Co and Ni, followed by precipitation of hydrous ferric oxide further downgradient, and subsequent sorption of Ba and Sr, and to a lesser extent, Co and Ni. Although these siderite and hydrous ferric oxide zones promote sorption of Ba, Sr, Co, and Ni, these trace element masses may be remobilized via changing geochemical conditions due to natural attenuation of bioavailable organic matter.

Although long-term monitored natural attenuation is an effective strategy for reducing the concentration of organic contaminants in aquifers, it results in secondary consequences in the form of trace element mobilization into groundwater. In this study of the Bemidji site, Ba^{2+} and

Ni^{2+} groundwater concentrations exceeded WHO guidelines and EPA health advisory levels, and are associated with health risks, including increased risk of high blood pressure (for Ba^{2+}; WHO report), gastrointestinal issues, and skin irritation (for Ni^{2+}; WHO report). Furthermore, simultaneous exposure to Ba^{2+} and As in drinking water is correlated with increased effects of As toxicity (Kato et al., 2013).

Last, it is important to note that the trace elements mobilized into groundwater as a result of natural attenuation are partially dependent on the trace elements initially present in the aquifer matrix. In this study, Ba, Sr, Co, and Ni mobilization are documented because they were present (albeit at low concentrations) in the aquifer matrix. However, the mobilization mechanism is not specific to Ba, Sr, Co, and Ni, and is likely to affect any trace elements associated with bioavailable Fe(III) in an aquifer. For example, other toxic trace elements (e.g. cadmium) were nondetectable in Bemidji aquifer sediments, but it is possible that an aquifer with higher levels of naturally occurring cadmium in sediment is vulnerable to unsafe levels of cadmium in drinking water if reducing conditions are established (e.g., following organic contamination). As such, this study highlights the importance of monitoring inorganic contaminants, and particularly trace elements, at organic contaminant sites.

Acknowledgments

I would like to thank the team of scientists at the USGS Minnesota Water Science Center and other participants in the summer 2019 Bemidji field season, including Jared Trost for field site coordination, Brent Mason and Andrew Berg for core collection, Jeanne Jaeschke and Paul Youngblood for help collecting samples, and Jennifer McGuire and Dalma Martinović-Weigelt for guidance in fieldwork approaches. Jeanne Jaeschke and Adam Mumford at the USGS generously provided ICP analyses. Isabelle Cozzarelli provided research guidance and valuable insights into the geochemistry and history of science at the Bemidji site. I am also grateful to Gerard Beaudoin, Brittany Long, and Frank Healy at Trinity University for lending their lab equipment and analytical expertise to this project, and to Glenn Kroeger for his explanation of modeling best practices and his feedback on earlier drafts of this thesis. Most importantly, I would like to express my gratitude towards Brady Ziegler for advising me on this thesis project.

This project was supported by Trinity University through the Hixon Environmental Studies Fellowship and Mach Family Research Fellowship. Groundwater chemistry data associated with this project is found at: https://mn.water.usgs.gov/projects/bemidji/data/. Sediment data will be available in a forthcoming data release.

References

Amirbahman, A., Kent, D.B., Curtis, G.P., and Davis, J.A., 2006, Kinetics of sorption and abiotic oxidation of arsenic(III) by aquifer matericals: *Geochimica et Cosmochimica Acta* vol. 70, p. 533-547, doi: https://doi.org/10.1016/j.gca.2005.10.036.

Baedecker, M.J., Cozzarelli, I.M., and Eganhouse, R.P., 1993, Crude oil in a shallow sand and gravel aquifer--III. Biogeochemical reactions and mass balance modeling in anoxic groundwater: *Applied Geochemistry* vol. 8, p. 569-586.

Bennett, P.C., Siegel, D.E., Baedecker, M.J., and Hult, M.F., 1993, Crude oil in a shallow sand and gravel aquifer--I. Hydrogeology and inorganic geochemistry: *Applied Geochemistry* vol. 8, p. 529-549.

Center for Disease Control: Toxicological Profile for Barium and Barium Compounds: https://www.atsdr.cdc.gov/ToxProfiles/tp24-c1.pdf.

Center for Disease Control: Toxicological Profile for Nickel and Nickel Compounds: https://www.atsdr.cdc.gov/ToxProfiles/tp15-c6.pdf.

Charlet, L., Wersin, P., and Stumm, W., 1990, Surface charge of MnCO3 and FeCO3: *Geochimica et Cosmochimica Acta* vol. 54, p. 2329-2336.

Cozzarelli, I.M., Bekins, B.A., Baedecker, M.J., Aiken, G.R., Eganhouse, R.P., and Tuccillo, M.E., 2001, Progression of natural attenuation processes at a crude-oil spill site: I. Geochemical evolution of the plume: *Journal of Contaminant Hydrology* vol. 53, p. 369-385.

Cozzarelli, I., Schreiber, M.E., Erickson, M.L., and Ziegler, B.A., 2016, Arsenic Cycling in Hydrocarbon Plumes: Secondary Effects of Natural Attenuation: *Groundwater*, doi: 10.1111/gwat.12316.

Crow, S.A., O'Neill, A.H., Weisener, C.G., Kulczycki, E., Fowle, D.A., and Roberts, J.A., 2007, Reductive Dissolution of Trace Metals from Sediments: *Geomicrobiology Journal* vol. 24, p. 157-165, doi: 10.1080/01490450701457329.

deLemos, J.L., Bostick, B.C., Renshaw, C.E., Sturup, S., and Feng, X., 2006, Landfill-stimulated iron reduction and arsenic release at the Coakley Superfund Site (NH): *Environmental Science & Technology* vol. 40, p. 67-73, doi: https://doi.org/10.1021/es051054h.

Durocher, J.L., and Schindler, M., 2011, Iron-hydroxide, iron-sulfate and hydrous-silica coatings in acid-mine tailings facilities: A comparative study of their trace-element composition: *Applied Geochemistry* vol. 26, p. 1337-1352, doi: https://doi.org/10.1016/j.apgeochem.2011.05.007.

Dzombak, D.A., and Morel, F.M.M., 1990, Surface Complexation Modeling: Hydrous Ferric Oxides: New York, John Wiley & Sons, Inc., 401 p.

Environmental Protection Agency, 2018, 2018 Edition of the Drinking Water Standards and Health Advisories Tables: https://www.epa.gov/sites/production/files/2018-03/documents/dwtable2018.pdf.

Erickson, M.L., and Barnes, R.J., 2005, Glacial sediment causing regional-scale elevated arsenic in drinking water: *Groundwater* vol. 43, p. 796-805.

Essaid, H.I., Bekins, B.A., Herkelrath, W.N., and Delin, G.N., 2009, Crude Oil at the Bemidji Site: 25 Years of Monitoring, Modeling, and Understanding: *Groundwater*, doi: 10.1111/j.1745-6584.2009.00654.x.

Frierdich, A.J., and Catalano, J.G., 2011, Controls on Fe(II)-Activated Trace Element Release from Goethite and Hematite: *Environmental Science & Technology*, vol. 46, p. 1519-1526, doi: dx.doi.org/10.1021/es203272z.

Grubbs, F.E., 1950, Sample criteria for testing outlying observations: *Annals of Mathematical Statistics* vol. 21, p. 27-58.

Kato, M., Kumasaka, M.Y., Ohnuma, S., Furuta, A., Kato, Y., Shekhar, H.U., Kojima, M., Koike, Y., Thang, N.D., Ohgami, N., Ly, T.B., Jia, X., Yetti, H., Naito, H., Ichihara, G., and Yajima, I., 2013, Comparison of Barium and Arsenic Concentrations in Well Drinking Water and in Human Body Samples and a Novel Remediation System for These Elements in Well Drinking Water: *PLoS One* vol. 8, doi: 10.1371/journal.pone.0066681.

Lovley, D.R., Baedecker, M.J., Lonergan, D.J., Cozzarelli, I.M., Phillips, E.J.P., and Siegel, D.J., 1989, Oxidation of aromatic contaminants coupled to microbial iron reduction: *Nature* vol. 339, p. 297-300.

Murphy, F., and Herkelrath, W., 1996, A sample-freezing drive shoe for a wire line piston core sampler: *Groundwater Monitoring & Remediation* vol. 16, p. 86-90.

Ng, G.-H.C., Bekins, B.A., Cozzarelli, I.M., Baedecker, M.J., Bennett, P.C., and Amos, R.T., 2014, A mass balance approach to investigating geochemical controls on secondary water quality impacts at a crude oil spill site near Bemidji, MN: *Journal of Contaminant Hydrology* vol. 164, p. 1-15, doi: https://doi.org/10.1016/j.jconhyd.2014.04.006.

Ramos Ramos, O.E., Rotting, T.S., French, M., Sracek, O., Bundschuh, J., Quintanilla, J., and Bhattacharya, P., 2014, Geochemical processes controlling mobilization of arsenic and trace elements in shallow aquifers and surface waters in the Antequera and Poopó mining regions, Bolivian Altiplano: *Journal of Hydrology*, doi: http://dx.doi.org/10.101016/j.hydrol.2014.08.019.

Small, T.D., Warren, L.A., and Ferris, F.G., 2001, Influence of ionic strength on strontium sorption to bacteria, Fe(III) oxide, and composite bacteria-Fe(III) oxide surfaces: *Applied Geochemistry* vol. 16, p. 939-946, doi: https://doi.org/10.1016/S0883-2927(00)00065-2.

Soderlund, M., Ervanne, H., Muuri, E., and Lehto, J., 2019, The sorption of alkaline earth metals on biotite: *Geochemical Journal* vol. 53, p. 223-234, doi: https://doi.org/10.2343/geochemj.2.0561.

Tuccillo, M.E., Cozzarelli, I.M., and Herman, J.S., 1999, Iron reduction in the sediments of a hydrocarbon-contaminated aquifer: *Applied Geochemistry* vol. 14, p. 655-667.

US EPA: Drinking Water Contaminant Candidate List (CCL) and Regulatory Determination, url: https://www.epa.gov/ccl.

US EPA: Secondary Drinking Water Standards: Guidance for Nuisance Chemicals, url: https://www.epa.gov/sdwa/secondary-drinking-water-standards-guidance-nuisance-chemicals.

USGS Minnesota Water Science Center: Bemidji Crude-Oil Research Project, url: https://mn.water.usgs.gov/projects/bemidji/index.html.

World Health Organization, 2011, Guidelines for Drinking-water Quality: Fourth edition: https://apps.who.int/iris/bitstream/handle/10665/44584/9789241548151_eng.pdf?sequence=1.

Zachara, J.M., Kukkadapu, R.K., Gassman, P., Dohnalkova, A., and Fredrickson, J.K., 2004, Biogeochemical transformation of Fe minerals in a petroleum-contaminated aquifer: *Geochimica et Cosmochimica Acta* vol. 68, no. 8, p. 1791-1805, doi: 10.1016/j.gca.2003.09.022.

Ziegler, B.A., McGuire, J.T., and Cozzarelli, I.M., 2015, Rates of As and trace-element mobilization caused by Fe reduction in mixed BTEX-ethanol experimental plumes: *Environmental Science & Technology* vol. 49, p. 13179-13189, doi: https://doi.org/10.1021/acs.est.5b02341.

Ziegler, B.A., Schreiber, M.E., and Cozzarelli, I., 2017, The role of alluvial aquifer sediments in attenuating a dissolved arsenic plume: *Journal of Contaminant Hydrology* vol. 204, p. 90-101, doi: https://doi.org/10.1016/j.jconhyd.2017.04.009.

Ziegler, B.A., Schreiber, M.E., Cozzarelli, I., and Ng, G.-H.C., 2017, A mass balance approach to investigate arsenic cycling in a petroleum plume: *Environmental Pollution* vol. 231, p. 1351-1361, doi: https://doi.org/10.1016/j.envpol.2017.08.110.